Applied Catalysis B: Environmental 96 (2010) 10–17

Contents lists available at ScienceDirect

Applied Catalysis B: Environmental

journal homepage: www.elsevier.com/locate/apcatb

Inhibition of nZVI reactivity by magnetite during the reductive degradation of 1,1,1-TCA in nZVI/magnetite suspension

Sungjun Bae, Woojin Lee *

Department of Civil and Environmental Engineering, Korea Advanced Institute of Science and Technology, 373-1 Guseong-Dong, 335 Gwahangno, Yuseong-Gu, Daejeon 305-701, Republic of Korea

ARTICLE INFO

Article history:
Received 15 September 2009
Received in revised form 26 January 2010
Accepted 28 January 2010
Available online 4 February 2010

Keywords:
Nano-sized zero-valent iron (nZVI)
Magnetite
Reductive degradation
1,1,1-Trichloroethane
nZVI inhibition

ABSTRACT

We demonstrated that the reactivity of nano-sized zero-valent iron (nZVI) can be inhibited by magnetite for the reductive degradation of 1,1,1-trichloroethane (1,1,1-TCA) in nZVI/magnetite suspension under low content of nZVI. A remarkable reductive degradation of 1,1,1-TCA (0.289 h^{-1}) was observed in nZVI (0.01 g/24 mL) suspension in 5 h, while no significant degradation was observed in nZVI (0.01 g)/magnetite (0.5 g) suspension in 80 h. The reductive dechlorination of 1,1,1-TCA in the nZVI/magnetite suspension started as the content of nZVI increased to 0.02 g. The slope of rate constant increase with respect to the nZVI content for nZVI suspension (17.67 g^{-1} h^{-1}) was greater than that for nZVI/magnetite suspension (14.89 g^{-1} h^{-1}) at the nZVI content between 0 and 0.1 g/24 mL. No significant difference in the inhibition of nZVI reactivity by magnetite was observed in the pH range of 6–9. Surface analyses using transmission electron microscopy and X-ray photoelectron spectroscopy revealed that the significant increase of Fe(II) on the magnetite surface was due to an electron transfer from nZVI on its surface resulting in the inhibition of nZVI reactivity for the reductive degradation of 1,1,1-TCA in the nZVI/magnetite suspension.

1. Introduction

Zero-valent iron (ZVI) technology has been extensively studied and developed for the treatment of soil and groundwater contaminants such as halogenated organics and inorganic chemicals [1–9]. Reductive dechlorination of halogenated organics (carbon tetrachloride (CT), dichloroethylene (DCE), and trichloroethene (TCE)) by ZVI has been well-known [1,9,10]. The successful oxidation of phenol and reduction of inorganics (nitrate, nitrite, and Cr(VI)) by commercial ZVI have been widely reported [7,11]. The reductive degradation kinetics of the contaminants has been accelerated by the use of bimetallic ZVI coated with Pd, Ni, Pt, Cu, and Ag [12–16]. Bimetallic Pd/Fe(0) has been reported to reductively degrade mono- and dichlorobenzenes and pentachlorophenol faster than Fe(0) [12,15]. It has been known to reductively dechlorinate persistent monochlorobiphenyls [17]. Ag/Fe(0) has also shown significant reductive dechlorination of tetra-, penta-, and hexachlorobenzenes [13]. Recently, nano-sized ZVI (nZVI) has attracted an attention due to its enhanced reactivity to better degrade the soil and groundwater contaminants [3,5,6]. It has been reported that the synthesis of nZVI by borohydride reduction resulted in the formation of spherical nZVI particles covered by a shell or core structure [4,18]. The hydrous iron oxide layer called "core–shell structure of nZVI" can produce sites for chemical complex formation resulting in fast adsorption of nickel and metal ions on the nZVI surface [19]. The reductive degradation of chlorinated aliphatics (1,1,1-trichloroethane (1,1,1-TCA), vinyl chloride, DCE, TCE, tetrachloroethene, chloroform, hexachloroethane, and pentachloroethane (PCA)) [3,5,8] and aromatics (*p*-chlorophenol and polychlorinated biphenyls) [6,20,21] by nZVI has shown much faster degradation kinetics than that by ZVI due to higher density of reactive sites on the nZVI surface. The effect of target contaminant concentration and suspension pH on the reactivity of nZVI has been reported [5,22]. No significant change has been observed in the kinetic rate constant of PCA as its concentration increased from 0.02 to 0.13 mM [5], while the rate constant of TCE increased as the pH decreased from 8.9 to 6.5 [22].

ZVI studies mixed with soil minerals were identified to enhance the reaction rate for reductive immobilization of Cr(VI) and oxidation by Fenton system [23–25]. Variety of aluminosilicate minerals (kaolinite and montmorillonite) and feldspar provides protons as electron acceptors to enhance the reduction of Cr(VI) [23]. The reduction of Cr(VI) by ZVI was also enhanced by the addition of magnetite (Fe_3O_4) showing higher Cr(VI) removal efficiency than that by ZVI or magnetite [24]. It has been reported that reductive dechlorination of CT and TCE by ZVI can be inhibited by the addition of natural organic matter (NOM) due to the

* Corresponding author. Tel.: +82 42 350 3624; fax: +82 42 350 3610.
E-mail addresses: bsj1003@kaist.ac.kr (S. Bae), woojin_lee@kaist.ac.kr (W. Lee).

0926-3373/$ – see front matter © 2010 Elsevier B.V. All rights reserved.
doi:10.1016/j.apcatb.2010.01.028

competition between contaminants and NOM for reactive surface sites of ZVI [26,27]. Iron hydroxide precipitants formed on nZVI surfaces at high suspension pH have been known to inhibit nZVI reactivity during the reductive transformation [28]. The amount of nZVI applied to contaminated sites for a successful remediation is usually much greater than that determined by a chemical stoichiometric estimation. This is because its reactivity can be limited or even inhibited by a variety of oxidants already existed (e.g., natural iron-bearing soil minerals) and/or produced (e.g., iron oxides formed on the nZVI surfaces) during the reductive degradation in natural and engineered systems. Therefore, identification of the inhibition mechanism on the reactivity of nZVI by the soil minerals is very important to produce basic knowledge for the development of effective and cost-efficient novel remediation technology. However, no significant research has been conducted to identify the inhibition of nZVI by iron-bearing soil minerals already existed and/or produced during the reductive dechlorination of chlorinated organics to date.

In this study, we have investigated the inhibition of nZVI reactivity by iron oxide for the reductive dechlorination of chlorinated organic. 1,1,1-TCA was selected as a representative chlorinated chemical extensively used before the Montreal Protocol [29] and magnetite was selected as a representative iron oxide. Batch kinetic tests were conducted to characterize the inhibition of nZVI reactivity by magnetite and to investigate the effect of nZVI loading and suspension pH on its inhibition during the reductive degradation of 1,1,1-TCA. Finally, surface spectroscopic analyses were carried out to explore the inhibition mechanism of nZVI on the surface of magnetite.

2. Experimental

2.1. Chemicals

Chemicals used in the experiment were 1,1,1-TCA (99.5%, Sigma), ferric chloride (98%, Sigma), ferrous chloride (99%, Sigma), ferric nitrate (98%, Sigma), sodium hydroxide (95%, Junsei, Japan), and sodium borohydride (99%, Sigma). Acetone (99.9%, Merck) used for nZVI washing, hexane (99.9%, Merck) for extractant, and methanol (99.9%, Merck) for the preparation of 1,1,1-TCA stock solution were all HPLC grade. Buffers used were 2-(N-morpholino) ethanesulfonic acid (MES, $pK_a = 6.10$, for pH 6, Sigma), 3-(N-morpholino) propanesulfonic acid (MOPS, $pK_a = 7.20$, for pH 7, Sigma), trizma (tris, $pK_a = 8.06$, for pH 8) mixture of tris (hydroxymethyl) aminomethane (99.8+%, Sigma) and trizma hydrochloride (99%, Sigma), and N-(tris(hydroxymethyl)methyl)-3-aminopropanesulfonic acid (TAPS, $pK_a = 8.40$, for pH 9, Sigma). Deaerated deionized water (DDW) was prepared using ultra-pure water (18 MΩ cm) purged by N_2 for 4 h and stored in an anaerobic chamber filled with 95% N_2 and 5% H_2 (Coy Laboratory Products Inc.).

2.2. Synthesis of nano-sized iron and magnetite

nZVI was synthesized by reducing 0.11 M $FeCl_3 \cdot 6H_2O$ with 0.9 M $NaBH_4$ solution, modifying Wang's method [6]. The precipitates in the solution were washed with DDW twice by centrifuging for 10 min at 3000 rpm, followed by acetone. nZVI was dried in anaerobic box flowed N_2 gas and stored in the anaerobic chamber. Magnetite (Fe_3O_4) was synthesized by modifying Taylor's method [30]. 0.03 M $Fe(NO_3)_3 \cdot 9H_2O$ was mixed in a reactor containing 0.3 M $FeCl_2 \cdot 4H_2O$. pH was increased and adjusted by the addition of 2 M NaOH during the mixing of suspension where air was bubbled at a constant flow rate (200 mL/min). The magnetite synthesis stopped when the pH was kept constant at 7.2. The precipitates in the suspension were washed 3 times using DDW, freeze-dried, and stored in the anaerobic chamber. The purity and identity of magnetite were investigated by X-ray diffraction (XRD).

2.3. Experimental procedures

24 mL of amber glass vials sealed with three-layered septum system (PTFE film, lead foil, and PTFE film lined with rubber septum) was used as anaerobic batch reactors for the characterization of reaction kinetics. All the experimental procedures were conducted in the anaerobic chamber. Exact amounts of nZVI (0.01 g) and magnetite (0.5 g) were transferred to the vials. MOPS buffer solution was poured into each vial without headspace to keep suspension pH constant at 7. The vials were sealed with the septum system, mixed by hand, and stood for 30 min for an interaction between nZVI and magnetite in the suspensions. 1,1,1-TCA stock solution in methanol (243 mM) was prepared at each test and its aliquot amount was (10 μL) spiked to each reactor by a gastight syringe (Hamilton) to start the reductive dechlorination. The vials were rapidly taken out of the anaerobic chamber, mounted on a tumbler, and mixed at 7 rpm at room temperature (25 ± 0.5 °C). The degradation kinetics of 1,1,1-TCA was obtained by monitoring its concentration in aqueous solution at each sampling time. Controls (50 mM of buffer solution without nZVI and magnetite) were prepared to evaluate a loss of target compound due to sorption and volatilization and tested under the same experimental conditions described above.

Five different levels of nZVI (0.01, 0.02, 0.04, 0.05 and 0.1 g) were used to investigate the effect of nZVI loading during the reductive dechlorination of 1,1,1-TCA with same amount of magnetite (0.5 g). To investigate the pH effect on the inhibition of nZVI reactivity during the reductive dechlorination, four different biological buffers of which pH range is 6.0–9.0 were introduced to the vials with nZVI (0.01 g) and magnetite (0.5 g). Unless stated otherwise, this parametric study followed the same experimental setup and procedures described above.

Batch kinetic experiment was conducted to investigate the degradation kinetics of 1,1,1-TCA by magnetite with Fe(II) addition. This was intended to simulate the inhibition of nZVI by magnetite during the degradation of 1,1,1-TCA and to confirm the inhibition during the reaction time by comparing the dechlorination kinetics of 1,1,1-TCA by magnetite with Fe(II) to that by nZVI/magnetite. An exact amount (1 mL) of $FeCl_2$ (540 mM) corresponding to the electron equivalent of nZVI was spiked to the vials containing 0.5 g magnetite. The resulting Fe(II) concentration was 22.5 mM, which is electronically equivalent to 7.5 mM Fe(0) (0.01 g/24 mL) under the assumption that Fe(0) can be fully oxidized to Fe(III). The experiment was conducted by following the experimental procedure and conditions used for the characterization experiment above.

2.4. Analytical procedures

The measurement of 1,1,1-TCA was performed by a Hewlett Packard 5890 gas chromatograph (GC) mounted with an electron capture detector and a HP-5 column (30 m × 0.32 mm × 0.25 μm). The temperature of injector and detector was 175 and 200 °C, respectively and oven temperature was isothermal at 80 °C. To analyze 1,1,1-TCA in aqueous solution, the retrieved vials were centrifuged at 3000 rpm for 5 min. An aliquot amount of supernatant (50 μL) was transferred to 2 mL vial containing 1 mL of extractant (hexane with 0.01 mM 1,2-dibromopropane as an internal standard). Extraction was conducted by mixing the vial on an orbital shaker for 30 min at 200 rpm and 1 μL of extractant was automatically injected into the GC injector with a split ratio of 5:1.

To identify the inhibition mechanism of nZVI in the presence of magnetite, surface analyses were carried out by X-ray photoelectron spectroscopy (XPS), transmission electron microscopy and energy dispersive X-ray (TEM–EDX), and scanning electron microscopy (SEM). The change of chemical binding of iron species on the surface of magnetite was obtained by XPS analysis. Three different samples (nZVI, magnetite, and nZVI/magnetite mixture) were equilibrated in MOPS buffer solution at pH 7 for 30 min. The solid samples were dried under an anaerobic condition for 24 h. The dried samples were carefully packed on XPS sampling template under the anaerobic condition to avoid surface oxidation of nZVI and magnetite. The XPS analysis was carried out using a MultiLab 2000 (Thermo Electron Co., UK) with an Al kα X-ray (1486.6 eV) having a source power of 200 W. Surface charging effects were corrected with C 1s peak at 285 eV as a reference. Shirley baseline and a Gaussian–Lorentzian peak shape were used for fitting the data. The narrow scanned spectra in the range of 278.1–297.1, 522.1–542.1, and 701.4–742.4 eV were used to identify the redox state of carbon, oxygen, and iron bound on the solid surfaces, respectively. XRD analysis of magnetite was conducted using Rigaku automated diffractometer using Cu KN radiation (D/MAX-RB). Two different samples (magnetite and nZVI/magnetite mixture) were equilibrated in MOPS buffer at pH 7 for 30 min. Other preparation procedure and drying condition were same to those for the XPS analysis above. No efforts were made to avoid the oxidation of nZVI during the XRD analysis. The scan range was 5–100° 2θ with a scan speed of $1^\circ\,min^{-1}$. To observe the morphology of nZVI and magnetite surfaces, SEM and TEM analyses were conducted by FE type SEM (XL30SFEG model, Philips) and TEM–EDX (Tecnai F20 model, Philips). Both analyses followed the preparation procedure for the XPS analysis above. For TEM analysis, a droplet of diluted nZVI and/or magnetite suspension was put on 300-mesh Cu TEM grids with a carbon film and dried in the anaerobic condition for 24 h. BET (Brunauer–Emmett–Teller) specific surface area of synthesized nZVI was measured by N_2 adsorption method using a Sorptomatic 1990 surface area analyzer (Thermo Fisher Scientific Inc.).

3. Results and discussion

3.1. Surface characteristics of nZVI and magnetite

TEM image shows that nZVI particles formed chain-like aggregates (Fig. 1(a)). It has been reported that nZVI single nanoparticles aggregate to micrometer-sized aggregates in 30 min, resulting in the formation of chain-like aggregates [31]. nZVI particle shown in the TEM image has a spherical shape of which diameter is in the range of 10–40 nm and its surface was covered by a 2.8–3.5 nm thick shell (Fig. 1(b and c)). The iron and oxygen contents on nZVI surface by XPS analysis were 16.16 and 83.84%, respectively (Fig. 2(a)). Specific surface area of nZVI synthesized in this study was $38.4 \pm 2.1\ m^2/g$, which is higher than that previously reported (33.2–35 m^2/g) due probably to smaller particle size (35–67 nm) [4,6,32]. Fig. 1(d) shows the surface images of magnetite by TEM. Magnetite shown in the TEM image also has a spherical shape, which was rounded by oxidation of $FeCl_2$ [33]. It was observed that

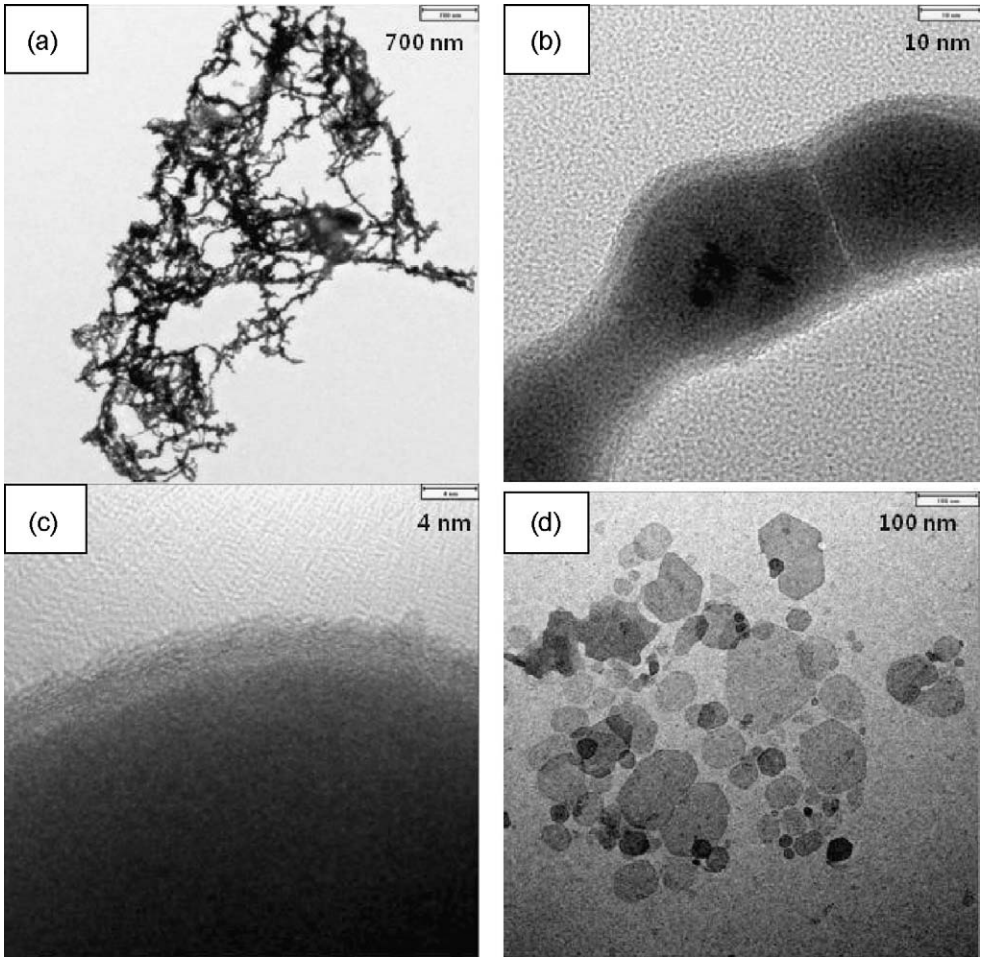

Fig. 1. (a) Chain-like aggregates of nZVI synthesized with borohydride; (b and c) core–shell structure of nZVI particles with 2.8–3.5 nm shell thickness; (d) spherical shape of magnetite synthesized by the oxidation of $FeCl_2$.

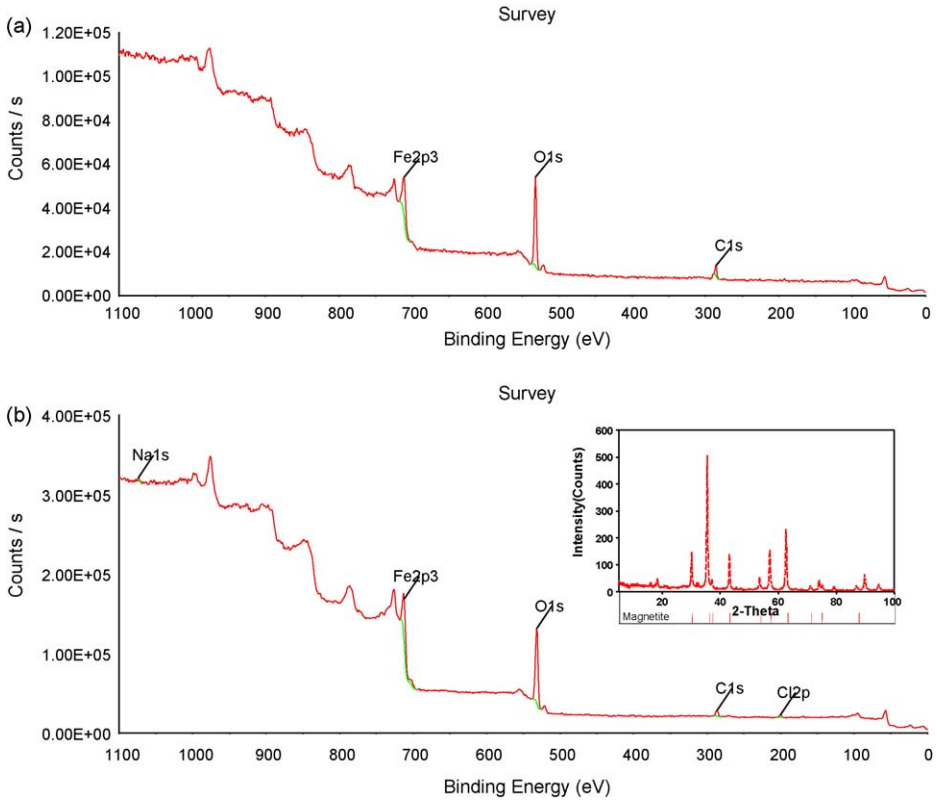

Fig. 2. (a) XPS spectrum of nZVI, atomic % of iron and oxygen are 16.16 and 83.84%, respectively. (b) XPS spectrum of magnetite, their atomic % are 23.44 and 76.56%, respectively. XRD diffractogram of magnetite was consistent to JCPDS standard (inset).

the magnetite was mostly composed of non-uniform particles with diameters of 50–150 nm. The iron and oxygen contents on synthesized magnetite surface by XPS analysis were 23.44 and 76.56%, respectively (Fig. 2(b)). XRD analysis was conducted to investigate the identity and purity of the magnetite. Its peak pattern was identical to that in a Joint Committee on Powder Diffraction Standards (JCPDS), indicating that the synthesized magnetite is pure $Fe^{(II)}Fe^{(III)}O_4$ (Fig. 2-inset).

3.2. Inhibition of nZVI reactivity by magnetite during the reductive dechlorination of 1,1,1-TCA

Fig. 3 shows the degradation kinetics of 1,1,1-TCA in nZVI suspension with and without magnetite at pH 7. Approximately, 79% of 1,1,1-TCA was degraded by nZVI in 5 h. 1,1,1-TCA may be rapidly transformed to 1,1-DCA as a major transformation product via hydrogenolysis pathway [5,16] and less amount of ethane, *cis*-2 butene, ethylene, and 2-butyne may also be produced during the dechlorination of 1,1,1-TCA, as previously reported [16]. No chlorinated products and non-chlorinated C_1 and C_2 hydrocarbons were measured in this research. Reaction kinetics for the reductive dechlorination of 1,1,1-TCA were able to be described by the following pseudo-first-order kinetic model:

$$\frac{dC_{L,TCA}}{dt} = -k_{obs,TCA} \cdot C_{L,TCA} \quad (1)$$

where $C_{L,TCA}$ is the concentration of 1,1,1-TCA in aqueous phase; $k_{obs,TCA}$ is the observed pseudo-first-order rate constant. The estimated kinetic rate constant of nZVI (0.01 g/24 mL) without magnetite was $0.289 \pm 0.019\ h^{-1}$, while that of nZVI (0.01 g/24 mL) with magnetite (0.5 g) was not able to be estimated because the reaction may not be kinetically controlled. Surface area-normalized rate constant (k_{SA}) was calculated by dividing the observed kinetic rate constant by measured nZVI surface area. The normalized rate constant of nZVI was $0.018 \pm 0.002\ L\ m^{-2}\ h^{-1}$, which is 8.3 times lower than that reported previously [5]. The lower reactivity of our nZVI may be due to different experimental conditions (e.g., mixing rpm, temperature, and aged nZVI) used for each experiment. The dechlorination kinetics of 1,1,1-TCA by magnetite without nZVI looked very slow and similar to that by control (Fig. 3 (inset)). This indicates that the addition of magnetite into nZVI suspension can inhibit nZVI reactivity for the reductive dechlorination of 1,1,1-TCA during the reaction time. The result contradicts to that previously

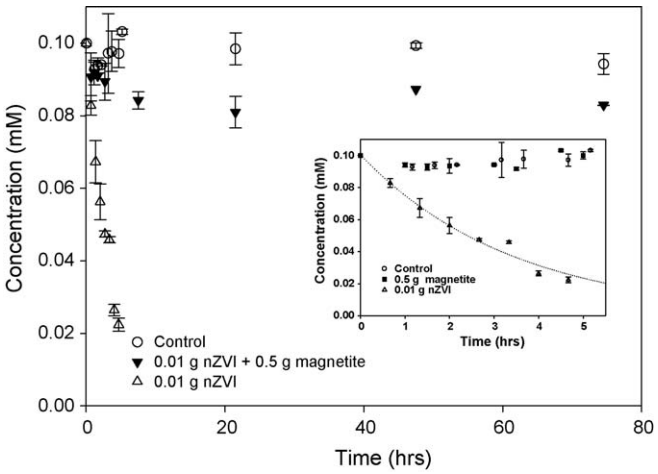

Fig. 3. Reductive degradation of 1,1,1-TCA by nZVI (0.01 g) in the absence and presence of magnetite (0.5 g) at pH 7 (MOPS). The initial concentration of 1,1,1-TCA was 0.1 mM. *Inset*: 79% of 1,1,1-TCA was degraded by nZVI in 5 h. A dashed line represents pseudo-first-order fit by Eq. (1). Error bars indicate standard deviation of duplicate samples.

reported for the reduction of Cr(VI) by nZVI with magnetite resulting in an accelerated reduction kinetics of Cr(VI) [24]. This may be caused by different reduction mechanism of Cr(VI) under different experimental conditions.

3.3. Effect of nZVI loading and pH on the inhibition of nZVI reactivity

Fig. 4(a) shows the dechlorination kinetic of 0.1 mM 1,1,1-TCA by five different contents of nZVI with magnetite (0.5 g) and three different contents of nZVI without magnetite. The results obtained from nZVI suspensions without magnetite indicated that the reductive dechlorination kinetics of 1,1,1-TCA was expedited as the increase of nZVI content (Table 1). The increase of kinetic rate constants with respect to nZVI addition can be appropriately explained by a linear fit shown in Fig. 4(b). A rapid increase in the rate constant was observed as increase of nZVI content. Slope of a linear regression line for nZVI in the whole range of nZVI content (0.01–0.1 g) was $17.67 \pm 1.398\ g^{-1}\ h^{-1}$, which implies the proportional increase of rate constant due to the increase of reactive nZVI surface. We normalized the slope value (0.01–0.1 g) by the nZVI surface area and obtained $0.010 \pm 0.001\ L\ m^{-2}\ h^{-1}$. In the presence of 0.5 g magnetite, no significant reductive dechlorination of 1,1,1-TCA has been observed in 0.01 g nZVI suspension. The dechlorination of 1,1,1-TCA was initiated as the nZVI loading increased by twice. The slope of a linear regression line for nZVI (0.02–0.1 g) with magnetite (0.5 g) was $14.89 \pm 1.546\ g^{-1}\ h^{-1}$. This indicates that nZVI suspension with magnetite was less reactive than nZVI for the reductive dechlorination of 1,1,1-TCA in the whole range of nZVI content tested here. Especially, at the lowest nZVI loading (0.01 g), its reactivity for the dechlorination of 1,1,1-TCA seemed to be significantly inhibited by the massive magnetite (Fig. 4(a)). This may be due to the loss of reductive capacity of nZVI by electron transfer between nZVI and magnetite after their mutual attraction. More detailed evidence for the electron transfer in the surface analyses section can help explain the inhibition mechanism described above. Magnetite surfaces could be fully covered by nZVI at high nZVI content. As its content increased, the amount of nZVI remnant may increase after saturation of magnetite surface and reach an equivalent reductive capacity to fully degrade 0.1 mM 1,1,1-TCA during the reaction time. This can be observed in nZVI suspensions with magnetite where the nZVI content was higher than 0.02 g.

Table 1
Observed pseudo-first-order rate constants (k_{obs}) and surface area-normalized rate constants (k_{SA}) for the reductive dechlorination of 1,1,1-TCA.[a]

Reductants	k_{obs} (h^{-1})[b]	k_{SA} ($L\,m^{-2}\,h^{-1}$)[c]
0.01 g nZVI	$2.89\ (\pm0.19) \times 10^{-1}$	$1.81\ (\pm0.154) \times 10^{-2}$
0.05 g nZVI	$1.08\ (\pm0.07) \times 10^{0}$	$6.75\ (\pm0.572) \times 10^{-2}$
0.1 g nZVI	$1.79\ (\pm0.06) \times 10^{0}$	$1.11\ (\pm0.072) \times 10^{-1}$
0.01 g nZVI + 0.5 g magnetite	–	–
0.02 g nZVI + 0.5 g magnetite	$6.53\ (\pm1.17) \times 10^{-2}$	–
0.04 g nZVI + 0.5 g magnetite	$4.97\ (\pm0.49) \times 10^{-1}$	–
0.05 g nZVI + 0.5 g magnetite	$6.70\ (\pm1.16) \times 10^{-1}$	–
0.1 g nZVI + 0.5 g magnetite	$1.30\ (\pm0.23) \times 10^{0}$	–

[a] Reaction conditions: 25 ± 0.5 °C, 24 mL reactor, pH 7 suspension.
[b] Uncertainties represent 95% confidence limits.
[c] k_{SA} values were calculated using nZVI surface area of 38.4 (±2.1) m^2/g.

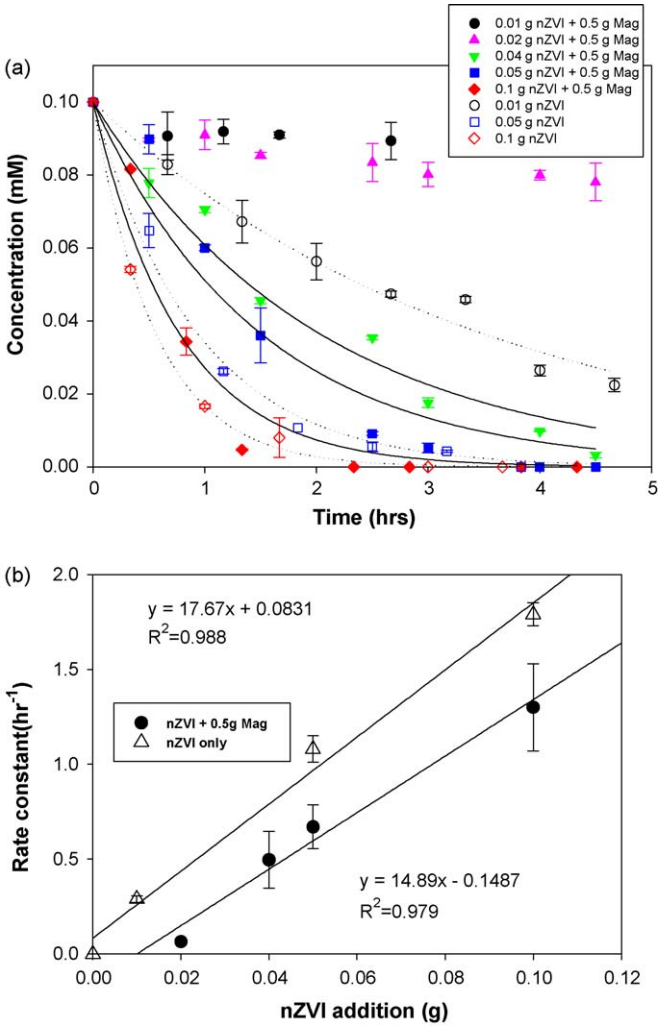

Fig. 4. (a) Effect of nZVI loading on the degradation of 0.1 mM 1,1,1-TCA in nZVI suspensions with magnetite (0.5 g) at pH 7. Solid/dashed lines represent pseudo-first-order fits by Eq. (1). (b) Change of kinetic rate constants for the degradation of 1,1,1-TCA with respect to nZVI loading at pH 7 (MOPS). Kinetic rate constants were fitted by a linear regression (solid line) with respect to nZVI loading (nZVI only: 0.01–0.1 g, nZVI/magnetite: 0.02–0.1 g). Error bars indicate standard deviation of duplicate samples.

Evaluation of pH effect on the removal of chlorinated contaminants by ZVI and iron-bearing soil minerals has been intensively conducted to date, because surface reactions at different pHs can significantly affect their dechlorination kinetics [5,7,34]. Fig. 5 shows the variation of kinetic rate constants for the dechlorination of 1,1,1-TCA by nZVI (0.01 g) with magnetite (0.5 g) at different suspension pHs. The kinetic rate constants decreased as the suspension pH increased in the range of pH 6–9, which is consistent with the results observed from the reductive degradation of 1,1,2,2-tetrachloroethane (1,1,2,2-TeCA), CCl_4, TCE, and Cr(VI) under different pHs [5,7,34,35]. It has been well-known that

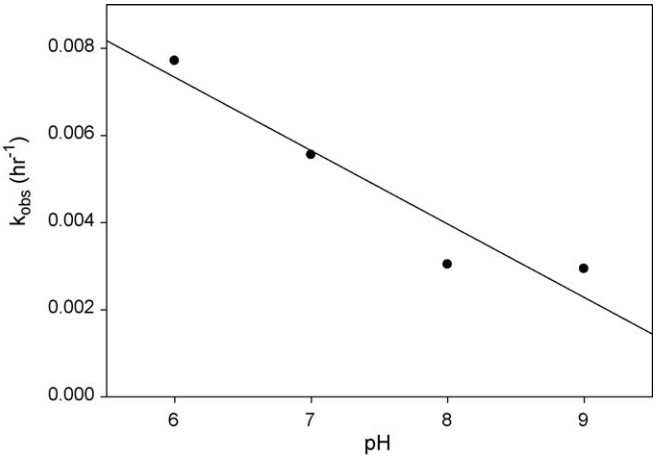

Fig. 5. Effect of pH (6–9) on the dechlorination kinetics of 1,1,1-TCA by nZVI (0.01 g) with magnetite (0.5 g).

the formation of iron oxide layers on nZVI surfaces can be inhibited at lower pH, resulting in the faster dechlorination kinetics of TCE [35], while, at high pHs, its surface complexes and precipitates (iron oxide and/or hydroxide) can be produced and limit its reactivity for the reductive dechlorination by surface passivation [28,35]. Surface charge of nZVI and magnetite at different suspension pH and their intrinsic magnetism could be significant factors which needs to be evaluated for the identification of the inhibition mechanism of nZVI and ultimate dechlorination kinetics of 1,1,1-TCA. Point of zero charge (PZC) of nZVI synthesized by borohydride reduction was observed at pH 8.3 and that of magnetite was done between 6.5 and 6.8 [36,37]. The surface of nZVI can be positively charged at pH 7 and 8, while that of magnetite can be negatively charged. This leads to surface attraction between nZVI and magnetite particles. At pH 6 and 9, both surfaces of nZVI and magnetite can be charged positively and negatively, thereby surface repulsion between the particles may occur. The reactivity of nZVI can be inhibited by magnetite when the surface attraction occurs at pH 7 and 8. However, this does not clearly explain the inhibition mechanism due to the attraction because the rate constant decreased as the suspension pH increased. An attraction by magnetism due to net interaction energy between magnetic nZVI and magnetite can predominate over that by different surface charges, when particle dipoles are oriented in a head-to-tail configuration [31]. The attraction between nZVI and magnetite due to their intrinsic magnetism can get over surface energy barrier for their rapid aggregation, which was estimated by extended DLVO theory [31]. Our experimental result on the inhibition mechanism and kinetics seemed to be more affected by the attraction due to the intrinsic magnetism rather than the different surface charges.

The estimated kinetic rate constants for the dechlorination by nZVI with magnetite in the range of pH 6–9 were 2–3 orders of magnitude smaller than those by ZVI without magnetite under similar experimental conditions previously reported [5,34]. A relationship between the rate constant and suspension pH was

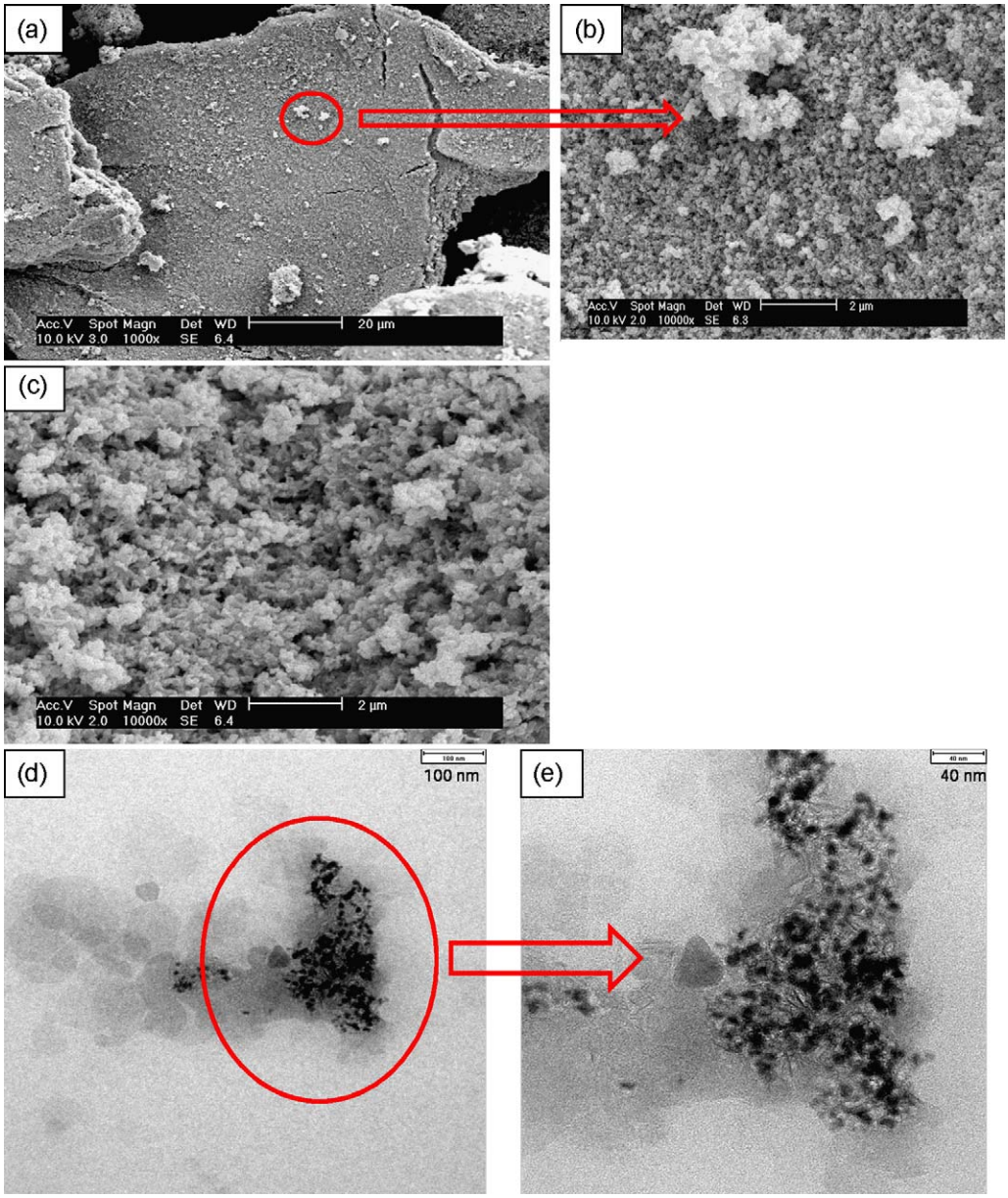

Fig. 6. (a and b) Different scale SEM images of nZVI/magnetite mixture: nZVI aggregates on the magnetite surfaces. (c) SEM image of nZVI. (d and e) TEM images of nZVI/magnetite mixture: nZVI aggregates (black dots) on the magnetite surfaces (grey spherical shape). Both SEM and TEM analyses used nZVI (0.05 g)/magnetite (2.5 g) suspension. For (c), solid nZVI particles were used for SEM analysis.

properly fitted by a linear regression ($R^2 = 0.91$). An estimated slope was 0.00168 h^{-1} pH^{-1}, which is approximately 143 and 643 times smaller than those of 1,1,2,2-TeCA and CCl_4 [5,34]. The results indicate that the pH change in the range of pH 6–9 did not significantly affect the dechlorination kinetics of 1,1,1-TCA implying that the inhibition of nZVI by magnetite was not significantly influenced by the pH change during the dechlorination of 1,1,1-TCA.

3.4. Surface analyses to identify the inhibition mechanism of nZVI by magnetite

Fig. 6(a) and (b) shows different scale SEM images demonstrating that different sized nZVI aggregates were sparsely bound on the magnetite surfaces. We have provided nZVI SEM image (Fig. 6(c)) to show nZVI aggregates and to compare them with nZVI aggregates on the magnetite surfaces. TEM images of nZVI/magnetite mixture clearly showed that nZVI aggregates (black dots) were associated on the surfaces of magnetite (grey colored spherical shape) (Fig. 6(d) and (e)). Magnetite has been well-known as a semiconductor with high conductivity (10^2 to 10^3 Ω^{-1} cm^{-1}) and narrow band gap (0.1 eV) showing its metallic characteristic [38,39]. Therefore, association of nZVI on the magnetite surface can easily occur by the magnetic attraction.

XPS analysis was conducted to check if the electron transfer occurs by identifying the change of redox state on magnetite surface before/after the addition of nZVI without spiking 1,1,1-TCA. Fig. 7 shows the narrow scans of Fe($2p_{3/2}$) on the surfaces of controls (nZVI and magnetite) and nZVI/magnetite mixture with their binding energies. The separation of magnetite and nZVI from the mixture was not conducted due to difficulties caused by their similar physico-chemical properties (magnetism and black color). Instead, we were able to selectively scan the magnetite surface from nZVI/magnetite mixture. The narrow region spectra for Fe($2p_{3/2}$) were composed of four identical peaks at 706.42, 709.32–709.59, 711–711.18, and 712.52–713.33 eV, respectively. It has been reported that the binding energies for Fe(0), Fe(II)–O, and Fe(III)–O were measured at 706.4, 709–709.5, and 711–714 eV, respectively [40–42]. As shown in Fig. 7, the peak intensities of Fe(III)–O of magnetite decreased considerably after the addition of nZVI, while that of Fe(II)–O increased. Table 2 shows surface percent composition of Fe species on the different solid surfaces. The surface of nZVI was composed of approximately 8.6% of Fe(0), 57.7% of Fe(II), and 33.7% of Fe(III). The oxidation of nZVI by atmospheric oxygen during the template setting on XPS seemed to contribute to the low Fe(0) and high Fe(III) contents on its surface. The addition of 0.01 g nZVI to magnetite increased the surface composition of Fe(II) species on magnetite by 2.3 times and decreased that of Fe(III) species by 2.9 times. The ratio of Fe(II) to Fe(III) on the surface of nZVI/magnetite mixture was 6.6 times greater than that of magnetite, indicating that surface-bound Fe(III) species on magnetite were reduced to Fe(II) by the electron transfer from nZVI on the magnetite surface. It has been reported that the spinel structure of magnetite can produce redox-versatile surface sites since it can accommodate both Fe(III) and Fe(II) [25,43]. Therefore, nZVI on the surfaces of magnetite could easily transfer electrons and reduce Fe(III) species on its surfaces during the reductive dechlorination of 1,1,1-TCA after physical contact. The electron transfer from ZVI to magnetite to reduce the surface-bound Fe(III) has been already well-known everywhere [24,25,43].

The surface-bound Fe(II) species on magnetite has been reported to be able to accelerate reductive degradations of Cr(VI) [24,44]. However, the reduced surface iron species on the

Table 2
Apparent surface compositions of Fe expressed as atomic % from X-ray photoelectron spectroscopy.[a].

	Fe(0)	Fe(II)	Fe(III)
nZVI/magnetite	–	77.40	22.60
Magnetite	–	34.19	65.81
nZVI	8.56	57.74	33.70

[a] Reaction conditions: 25 ± 0.5 °C, 24 mL reactor, pH 7 suspension, dried in an anaerobic chamber for 24 h. All sample preparations were conducted in the anaerobic chamber.

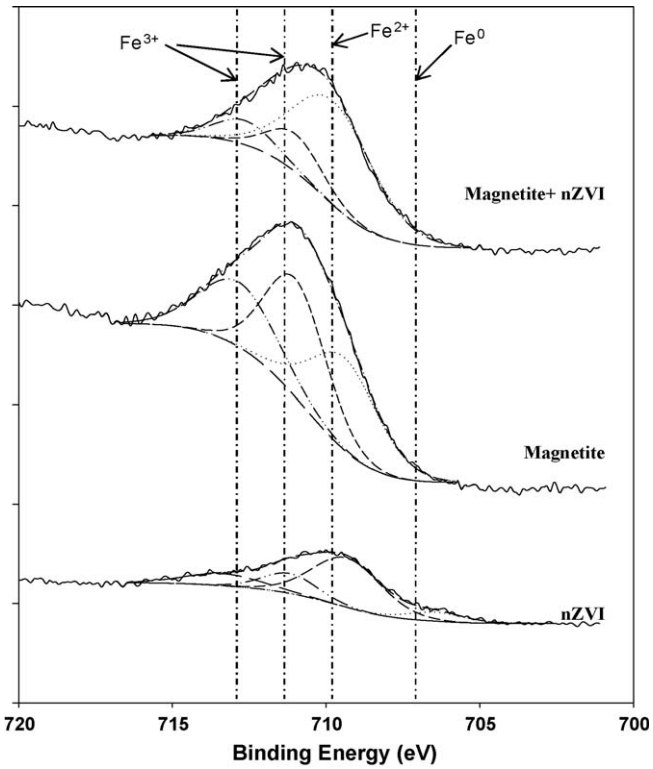

Fig. 7. XPS spectra for the narrow scan of Fe($2p_{3/2}$) on the surfaces of nZVI (0.01 g), magnetite (0.5 g), and nZVI (0.01 g)/magnetite (0.5 g) mixture with their binding energies.

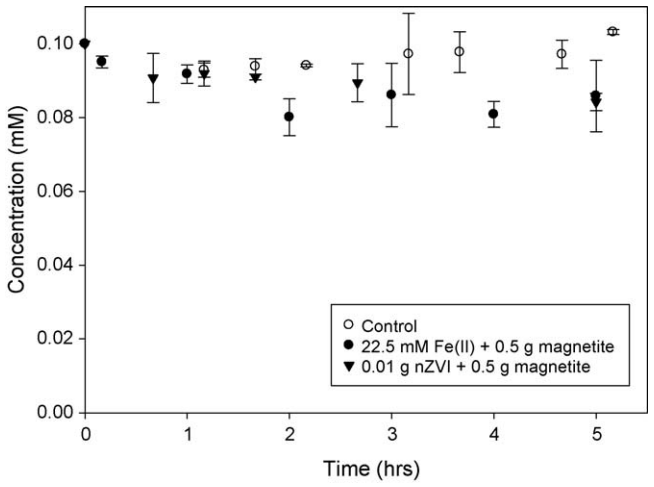

Fig. 8. Reductive degradations of 1,1,1-TCA by magnetite (0.5 g) with Fe(II) (22.5 mM) and by nZVI (0.01 g)/magnetite (0.5 g) mixture at pH 7 (MOPS). The initial concentration of 1,1,1-TCA was 0.1 mM. Control (no reductant) experiment was conducted under the same experimental conditions. Error bars indicate standard deviation of duplicate samples.

nZVI/magnetite mixture under low nZVI content were far less reactive than those previously reported or nZVI for the reductive degradation of 1,1,1-TCA during the reaction time. To investigate the reactivity of surface-bound Fe(II) on magnetite for the dechlorination of 1,1,1-TCA, an exact amount of ferrous iron (22.5 mM) equivalent to that of nZVI based on electron equivalent was added to the magnetite suspension and its dechlorination kinetics were compared to that of nZVI/magnetite mixture. No significant difference in the degradation kinetics was observed between the two samples in 5 h (Fig. 8), indicating that the surface-bound Fe(II) on magnetite did not play a significant role for the dechlorination of 1,1,1-TCA during the short reaction time. A minor dechlorination of *cis*-dichloroethylene and vinyl chloride by surface-bound Fe(II) species on magnetite has been observed in 100 days [45], which suggests that the dechlorination of 1,1,1-TCA by the Fe(II) on magnetite cannot be a kinetically controlled reaction in the short reaction time period studied in this research.

4. Conclusions

The research was conducted to investigate the inhibition effect of nZVI reactivity by magnetite on the reductive dechlorination of 1,1,1-TCA. In contrast to nZVI (0.01 g)/magnetite (0.5 g) suspension which showed no significant degradation in 80 h, 79% of 1,1,1-TCA was degraded in nZVI (0.01 g) suspension in 5 h. Based on the XPS analysis, the results imply that nZVI lost its reductive capacity by transferring electrons to magnetite surfaces resulting in the reduction of Fe(III) species on magnetite surfaces rather than to directly dechlorinate 1,1,1-TCA at low nZVI content. The results for the nZVI loading showed that reductive dechlorination of 1,1,1-TCA started as nZVI content increased to 0.02 g in the nZVI/magnetite suspension due to the increase in the amount of nZVI remnant after saturation of magnetite surface. No significant difference of rate constants on the pH effect for inhibition of nZVI reactivity may be caused by strong magnetic attraction between magnetite and nZVI rather than effect of PZC (i.e., different surface charges) on their surfaces. Based on the results of this study, we can propose the dechlorination mechanism of 1,1,1-TCA by nZVI/magnetite under the inhibited condition such as low nZVI dosage by three steps: (1) the attraction of nZVI to magnetite surface occurs by the magnetic attraction, (2) electrons transferred from nZVI are willing to reduce Fe(III) species to Fe(II) on magnetite surface rather than to reductively dechlorinate 1,1,1-TCA, and (3) after the equilibration time, the surface-bound Fe(II) on nZVI/magnetite mixture starts to dechlorinate 1,1,1-TCA at an extremely low dechlorination rate. Such an insignificant dechlorination of 1,1,1-TCA in nZVI/magnetite mixture seems to be due to the inhibition of nZVI reactivity for the dechlorination by the electron transfer from nZVI, otherwise it can be directly used for the dechlorination of 1,1,1-TCA as observed in nZVI suspension. The results obtained from this study can provide basic understanding to develop novel nZVI remediation technologies and apply them to the contaminated sites containing high contents of oxidized iron-bearing soil minerals and to operate developed nZVI technologies properly.

Acknowledgments

This research was supported by the Korea Research Foundation (KRF-2007-313-D00439) and partially supported by the Korean Ministry of Environment through the GAIA project.

References

[1] A.L. Roberts, L.A. Totten, W.A. Arnold, D.R. Burris, T.J. Campbell, Environ. Sci. Technol. 30 (1996) 2654–2659.
[2] P.G. Tratnyek, R.L. Johnson, Nano Today 1 (2006) 44–48.
[3] S. Choe, S.H. Lee, Y.Y. Chang, K.Y. Hwang, J. Khim, Chemosphere 42 (2001) 367–372.
[4] J.H. Kim, P.G. Trantnyek, Y.S. Chang, Environ. Sci. Technol. 42 (2008) 4106–4112.
[5] H. Song, E.R. Carraway, Environ. Sci. Technol. 39 (2005) 6237–6245.
[6] C.B. Wang, W.X. Zhang, Environ. Sci. Technol. 31 (1997) 2154–2156.
[7] M.J. Alowitz, M.M. Scherer, Environ. Sci. Technol. 36 (2002) 299–306.
[8] H. Song, E.R. Carraway, Appl. Catal. B: Environ. 78 (2008) 53–60.
[9] Y. Jiao, C. Qiu, L. Huang, K. Wu, H. Ma, S. Chen, L. Ma, D. Wu, Appl. Catal. B: Environ. 91 (2009) 434–440.
[10] T.L. Johnson, M.M. Scherer, P.G. Tratnyek, Environ. Sci. Technol. 30 (1996) 2634–2640.
[11] D.H. Bremner, A.E. Burgess, D. Houllemare, K.-C. Namkung, Appl. Catal. B: Environ. 63 (2006) 15–19.
[12] Y.H. Kim, E.R. Carraway, Environ. Sci. Technol. 34 (2000) 2014–2017.
[13] Y. Xu, W.X. Zhang, Ind. Eng. Chem. Res. 39 (2000) 2238–2244.
[14] B. Schrick, J.L. Blough, A.D. Jones, T.E. Mallouk, Chem. Mater. 14 (2002) 5140–5147.
[15] B.W. Zhu, T.T. Lim, Environ. Sci. Technol. 41 (2007) 7523–7529.
[16] J.P. Fennelly, A.L. Roberts, Environ. Sci. Technol. 32 (1998) 1980–1988.
[17] Y. Fang, S.R. Al-Abed, Appl. Catal. B: Environ. 78 (2008) 371–380.
[18] J.T. Nurmi, P.G. Tratnyek, V. Sarathy, D.R. Baer, J.E. Amonette, K. Pecher, C. Wang, J.C. Linehan, D.W. Matson, R.L. Penn, M.D. Driessen, Environ. Sci. Technol. 39 (2005) 1221–1230.
[19] X.Q. Li, W.X. Zhang, Langmuir 22 (2006) 4638–4642.
[20] R. Cheng, J.I. Wang, W.-X. Zhang, J. Hazard. Mater. 144 (2007) 334–339.
[21] G.V. Lowry, K.M. Johnson, Environ. Sci. Technol. 38 (2004) 5208–5216.
[22] Y. Liu, G.V. Lowry, Environ. Sci. Technol. 40 (2006) 6085–6090.
[23] R.M. Powell, R.W. Puls, Environ. Sci. Technol. 31 (1997) 2244–2251.
[24] F.D.S. Coelho, J.D. Ardisson, M.H. Araújo, F.C.C. Moura, R.M. Lago, E. Murad, J.D. Fabris, Chemosphere 71 (2008) 90–96.
[25] F.C.C. Moura, M.H. Araújo, R.C.C. Costa, J.D. Fabris, J.D. Ardisson, W.A.A. Macedo, R.M. Lago, Chemosphere 60 (2005) 1118–1123.
[26] P.G. Tratnyek, M.M. Scherer, B. Deng, S. Hu, Water Res. 35 (2001) 4435–4443.
[27] J. Klausen, P.J. Vikesland, T. Kohn, D.R. Burris, W.P. Ball, A.L. Roberts, Environ. Sci. Technol. 37 (2003) 1208–1218.
[28] M.M. Scherer, B.A. Balko, P.G. Balko, in: D. Sparks, T. Grundl (Eds.), Mineral Water Interfacial Reactions: Kinetics and Mechanisms, American Chemical Society, Washington, DC, 1998, pp. 301–322, ACS Symposium Series No. 715.
[29] D.J. Reed, in: M.H.-G. Kroschwitz (Ed.), Kirk–Othmer Encyclopedia of Chemical Technology, vol. 5, John Wiley & Sons, New York, 1993.
[30] R.M. Taylor, B.A. Maher, P.G. Self, Clay Miner. 22 (1987) 411–422.
[31] T. Phenrat, N. Saleh, K. Sirk, R.D. Tilton, G.V. Lowry, Environ. Sci. Technol. 41 (2007) 284–290.
[32] H.-L. Lien, W.-X. Lien, Colloid Surf. A 191 (2001) 97–105.
[33] U. Schwertmann, E. Murad, Clays Clay Miner. 38 (1990) 196–202.
[34] L.J. Matheson, P.G. Matheson, Environ. Sci. Technol. 28 (1994) 2045–2053.
[35] J.-L. Chen, S.R. Al-Abed, J.A. Ryan, Z. Li, J. Hazard. Mater. B83 (2001) 243–254.
[36] Y.-P. Sun, X.Q. Li, J. Cao, W. Zhang, H.P. Wang, Adv. Colloid Interface Sci. 120 (1–3) (2006) 47–56.
[37] R.M. Cornell, U. Schwertmann, The Iron Oxides: Structure, Properties, Reactions, Occurrence and Uses, 2nd, VCH, Weinheim, 2003.
[38] J.K. Leland, A.J. Bard, J. Phys. Chem. 91 (1987) 5076–5083.
[39] A.F. White, Rev. Miner. 23 (1990) 467–509.
[40] R. Devaux, D. Vouagner, A.M. De Becdelievre, C. Duret-Thual, Corros. Sci. 36 (1994) 171–186.
[41] M. Mullet, S. Boursiquot, M. Abdelmoula, J.-M. Genin, J.-J. Ehrhardt, Geochim. Cosmochim. Acta 66 (2002) 829–836.
[42] J.E. Thomas, C.F. Jones, W.M. Skinner, R.S.C. Smart, Geochim. Cosmochim. Acta 62 (1998) 1555–1565.
[43] F.C.C. Moura, G.C. Oliveira, M.H. Araújo, J.D. Ardisson, W.A.A. Macedo, R.M. Lago, Chem. Lett. 34 (2005) 1172–1173.
[44] Y. Jung, J. Choi, W. Lee, Chemosphere 68 (2007) 1968–1975.
[45] W. Lee, B. Batchelor, Environ. Sci. Technol. 36 (2002) 5147–5154.